Talanta 114 (2013) 283–290

Contents lists available at ScienceDirect

Talanta

journal homepage: www.elsevier.com/locate/talanta

Surface modified $BaTiO_3$ nanoparticles as the matrix for phospholipids and as extracting probes for LLME of hydrophobic proteins in *Escherichia coli* by MALDI–MS

Suresh Kumar Kailasa [a,b,c], Hui-Fen Wu [a,b,d,e,*]

[a] Department of Chemistry, National Sun Yat-Sen University, Kaohsiung, 80424, Taiwan
[b] Center for Nanoscience and Nanotechnology, National Sun Yat-Sen University, Kaohsiung, 80424, Taiwan
[c] Department of Chemistry, S.V. National Institute of Technology, Surat 395007, India
[d] Doctoral Degree Program in Marine Biotechnology, National Sun Yat-Sen University, Kaohsiung 80424, Taiwan
[e] School of Pharmacy, College of Pharmacy, Kaohsiung Medical University, 806, Kaohsiung, Taiwan

ARTICLE INFO

Article history:
Received 21 December 2012
Received in revised form
7 May 2013
Accepted 11 May 2013
Available online 20 May 2013

Keywords:
HOA-modified $BaTiO_3$ NPs
PLs
E. coli
FT-IR
TEM
MALDI–MS

ABSTRACT

In this paper, we report the dual function of 12-hydroxy octadecanoic acid (HOA)-modified barium titanate nanoparticles ($BaTiO_3$ NPs) as the matrix for phospholipids (PLs) and as hydrophobic affinity probes for liquid–liquid microextraction (LLME) of hydrophobic proteins in *Escherichia coli* prior to their identification by matrix-assisted laser desorption/ionization time-of-flight mass spectrometry (MALDI–MS). FT-IR, SEM and TEM were used for the characterization of the HOA-modified $BaTiO_3$ NPs. The surface modified $BaTiO_3$ NPs acted as multifunctional probes (as extracting probes and as the matrix) for the analysis of PLs by MALDI–MS. Compared to 2,5-dihydroxybenzoic acid (2,5-DHB), the HOA-modified $BaTiO_3$ NPs provided good PLs mass spectra with similar or improved signal-to-noise (S/N) ratio, which demonstrated the potentiality of HOA-modified $BaTiO_3$ NPs as a PLs purpose matrix. This method was found to be linear in concentration ranges of 1.0–5.0 μM and 1.0–10.0 μM for L-A-phosphatidyl-L-serine (PS) and L-A-phsophatidic acid sodium (PA) with correlation coefficient (R^2) values from 0.9905 to 0.9987. The detection limits were 0.20–0.35 μM and 0.25–0.40 μM for PS and PA, respectively. We also demonstrated the HOA-modified $BaTiO_3$ NPs as extracting and as preconcentrating probes for the LLME of hydrophobic proteins in *E. coli* prior to their identification by MALDI–MS. Thus, the surface modified $BaTiO_3$ NPs-assisted LLME coupled with MALDI–MS provides a simple methodology for the efficient extraction and determination of hydrophobic molecules in biological samples.

1. Introduction

Phospholipids are complex structures by combination of polar head groups and fatty acyl chains. PLs play key roles in many cellular functions and directly participate in membrane protein regulation and function. PLs serve as a cell fuel for the signaling of molecules in various biological tissues and play fundamental role in the transport of fat between gut and liver in mammalian digestion process. Therefore, PLs act as key components in wide variety of biological cell membranes and serve as the prime building blocks for all known life forms [1–4]. In view of their key diverse roles in biological pathway, various chromatographic methods such as thin-layer chromatography [5], high-performance liquid chromatography [6] and micellar electrokinetic chromatographic [7] methods have been used for the analysis of PLs in various samples. However, these methods required to use large amount of solvents, extensive purification procedures and long time for analysis.

Mass spectrometry (MS) is a powerful bioanalytical tool for the analysis of a wide variety of biomolecules in biological/complex samples with relatively high sensitivity. The development of two "soft ionization" techniques such as electrospray ionization (ESI) [8] and matrix-assisted laser desorption/ionization (MALDI) [9,10] introduced in the late 1980s, are superior tools for biomolecule analysis than those of the classical ionization methods such as electron impact and chemical ionization which can be applied to ionize only small and volatile molecules. Even though, ESI time-of-flight mass spectrometry (TOF–MS) is also a common tool for large biomolecule analysis [11], it requires time consuming and expensive separation devices such as HPLC and 2D gels prior to ESI–MS analysis. Besides, owing to sample injection step is required, the ESI–MS takes more sample cleanup steps and longer analysis time than the MALDI–MS. Within two decades,

* Corresponding author at: Department of Chemistry, National Sun Yat-Sen University, Kaohsiung, 80424, Taiwan. Tel.: +886 7 5252000x3955; fax: +886 7 5253908.
E-mail address: hwu@faculty.nsysu.edu.tw (H.-F. Wu).

0039-9140/$ - see front matter © 2013 Elsevier B.V. All rights reserved.
http://dx.doi.org/10.1016/j.talanta.2013.05.032

MALDI–MS has become a popular and versatile analytical tool for the analysis of a wide range of macromolecules such as proteins [12], bacteria [13] and clinical samples [14]. Since it has capability to desorb high molecular weight and thermolabile molecules with acceptable mass accuracy and sensitivity. However, the detection efficiencies of PLs by MALDI–MS are comparably low because of their structures with high number of alkyl chains, easily fragmentation during ionization by MS and lengthy sample preparation procedures [15]. Thus, several reports have investigated the use of various organic molecules including 4-nitroaniline/butyric acid [16], 2,5-dihydroxybenzoic acid (2,5-DHB) [17], and ionic liquid matrices (butyl ammonium-α-cyano-4-hydroxycinnamic acid (BA-CHCA), 1-methyl imidazolium-α-cyano-4-hydroxy-cinnamic acid (MI-CHCA)) [18] as possible MALDI matrices for PL analysis. Additionally, Harvey applied various organic acids including 1,4-dihydroxy-2-naphthoic acid, 3,7-dihydroxy-2-naphthoic acid, 4-hydroxycoumarin, 7-hydroxycoumarin, 7-hydroxycoumarin-4-acetic acid, 7,8-dihydroxy-6-methoxycoumarin, 3-hydroxypicolinic acid, 2,5-dihydroxyteraphthalic acid and 2,5-DHB as feasible MALDI matrices for PL analysis [19]. These matrices cause strong interferences with PLs mass spectra and required specific solvent system. This is due to these organic matrices are insoluble in water and small molecular weights ($<$ 1500 Da) [15] which are easily to be ionized to generate unwanted cluter ions.

In recent years, MALDI imaging mass spectrometry (IMS) has proven to be a powerful bioanalytical tool which enables to investigate PLs *in vitro* without sample pretreatments (extraction, purification and labeling) [20]. Therefore, various organic molecules such as CHCA-butylamine and 2,5-DHB-butylamine [21], 2,5-DHB [22], 2,5-DHB- and CHCA-piperidine [23], 4′,6-diamidino-2-phenylindole (DAPI), 2,6-dihydroxyacetophenone (DHAP) and 2,5-DHB [24] and 2,5-DHB [25] have been used as possible MALDI matrices for PL analysis. These approaches provide clean PLs mass spectra without sample pretreatment, but they need a suitable/specific matrix for the analysis of PLs in tissues by MALDI–IMS. Recently, the application of nanomaterials as MALDI matrices and to serve as extracting (affinity) probes for the analysis of a wide variety of molecules have been very successful [26,27]. Moreover, surface modified -Ag NPs [28], -Mg $(OH)_2$ NPs [29], -Au NPs [30,31] and -Ag_2Se NPs [32] have been used as effective extracting/preconcentrating probes for LLME of biomolecules prior to their identification by MALDI–MS. In these methods, functionalized NPs are used as affinity probes for the selective enrichment of target species at trace level. We describe here a new class of nanomaterials based on the functionalization of $BaTiO_3$ NPs with hydrophobic capping ligand for the efficient extraction and preconcentration of hydrophobic target species prior to their identification by MALDI–MS. The unique properties of $BaTiO_3$ NPs have been applied as alternative cellular nanovectors to study their cytocompatibility for cancer therapy [33]. Since the surface functionality of NPs provides well control on their physico-chemical properties to interact with various biomolecules (peptides, proteins, cell membrane lipids, and nucleic acids). Also, the hydrophobic liquid compounds have been used as initiators in nanostructure-initiator MS for effective desorption of analytes on the DIOS substrate [34]. In the current approach, we functionalized the $BaTiO_3$ NPs surfaces with the hydrophobic molecule (HOA) and used it as novel nanoprobes to act as the matrix for PLs (PS and PA) analysis and as hydrophobic affinity probes (via LLME) to extract the hydrophobic proteins from *Escherichia coli* prior to MALDI–MS analysis.

2. Experimental section

2.1. Chemicals

All chemicals were of the highest available purity grade and were used without further purification. $BaTiO_3$ NPs (~30 nm, 99%), 2,5-DHB, L-A-phosphatidyl-L-serine from bovine brain and L-A-phsophatidic acid sodium from egg yolk lecithin were obtained from Sigma-Aldrich (St. Louis, MO, USA). Capping agent (HOA) and 3,5-dimethoxy-4-hydroxycinnamic acid (SA) were purchased from Alfa Aesar, Ward Hill, MA 01835 USA. Hydrogen peroxide (35, wt%) was obtained from Showa Chemical Co., Japan. Deionized water (18 MΩ Milli-Q water system, Millipore Inc., Bedford, MA, USA) was used for the preparations of standard solutions.

2.2. Solutions

Stock solutions of PS (1.3 mM) and PA (1.4 mM) were prepared in chloroform and methanol (1:1, v/v). The stock solutions were further diluted to appropriate concentration with chloroform and methanol (1:1, v/v). 0.2 M of 2,5-DHB and 0.5 M of SA were prepared in 2:1 (v/v) of ACN-water that contained 0.1% of trifluoroacetic acid.

2.3. Bacteria growth

E. coli (12570) standard culture bacteria were obtained from Bioresource Collection and Research Center, Taiwan. Glassware and media were subjected to autoclave at 15 lbs of pressure for 15 min prior to bacteria culture. One colony of *E. coli* was carefully taken up from a freshly prepared, 24 h old streak plate culture using a sterile loop. The collected bacteria were cultured on Luria Broth Agar (LBA) plates for 24 h at 37 °C. The concentration of bacteria was checked by plate count method [35]. All microbiological experiments were performed in a Biosafety Level 1 cabinet (Nuaire, Plymouth, MN, USA).

2.4. Synthesis of surface modified $BaTiO_3$ NPs with HOA

Surfaced modified $BaTiO_3$ NPs were synthesized according to the literature procedure [36]. However, we slightly modified the procedure to prepare HOA capped $BaTiO_3$ NPs. Briefly, $BaTiO_3$ NPs (0.5 g) surfaces were hydroxylated by refluxing with 200 mL of H_2O_2 for 4 h at 106 °C. The hydroxylated $BaTiO_3$ NPs were filtered and then washed with deionized water twice. The hydroxylated $BaTiO_3$ NPs were directly added into 250 mL round bottom flask that contained 50 mL of 50% (v/v) aqueous alcohol along with 0.5 (w/v) of HOA. The reaction mixture was heated at 90 °C under vigorous stirring for 3 h. The reaction mixture was cooled to room temperature and HOA-modified $BaTiO_3$ NPs were treated with 1 N HCl until the pH became 5–6 in order to agglomerate the nanopowder and to facilitate NPs filtration. The surface modified $BaTiO_3$ NPs were washed with deionized water and acetone in sequence, for several times. The surface modified $BaTiO_3$ NPs were dried in vacuum oven for 24 h and then dispersed in toluene by ultrasonication for 10 min (Fig. 1).

2.5. HOA-modified $BaTiO_3$ NPs-assisted LLME for PLs and hydrophobic proteins

PLs and hydrophobic proteins were analyzed by using HOA-modified $BaTiO_3$ NPs-assisted LLME coupled with MALDI–MS. For PLs; 900 μL of PLs (PS and PA, 2.0 μM) were taken separately into 1.0 mL polyethylene vials. To this, 100 μL of HOA-modified $BaTiO_3$ NPs dispersed in toluene was added and then vortexed for 30 min at 900 rpm. The sample vials were kept on stand for 3 min to separate the NPs contained in organic layer and in aqueous layer. After that, 1 μL of HOA-modified $BaTiO_3$ NPs conjugated PLs (PS and PA) were directly deposited onto the MALDI plate, air-dried and then analyzed by MALDI–MS. For hydrophobic proteins in *E. coli*; 200 μL of cultured *E. coli* (1.5×10^8 cfu/mL) was taken into a 1.0 mL vial and then 200 μL of HOA-modified $BaTiO_3$ NPs

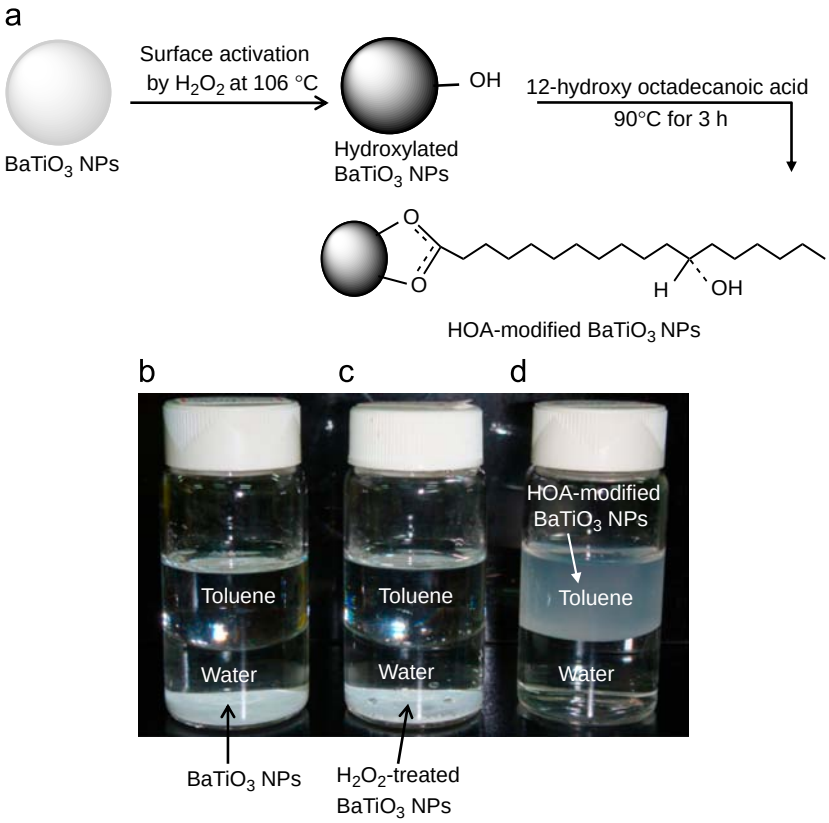

Fig. 1. (a) Schematic representation of the synthesis of HOA-modified $BaTiO_3$ NPs, (b) photographs of (b) as received $BaTiO_3$ NPs, (c) after H_2O_2-treated $BaTiO_3$ NPs and (d) dispersed HOA-modified $BaTiO_3$ NPs in toluene.

dispersed in toluene was added. The vials were vortexed for 30 min at room temperature. The sample vials were kept on stand for 3 min to the separate NPs contained in organic layer and in aqueous layers. Then, 1.0 μL of HOA-modified $BaTiO_3$ NPs-conjugated hydrophobic proteins (upper layer) was mixed with 1.0 μL of 0.5 M SA. Finally, 1.0 μL of above solution was placed on the MALDI target plate, dried at room temperature and then analyzed by MALDI–MS.

2.6. Instrumentation

The synthesized HOA-modified $BaTiO_3$ NPs were characterized by Fourier transform infrared (FT-IR) spectrometer (IFS-48, Bruker, Germany), scanning electron microscope (SEM) (JEOL-6400, JEOL, Tokyo, Japan) and transmission electron microscope (TEM) (TEM-3010, JEOL, Tokyo, Japan). All mass spectra were generated on a Bruker Daltonics Microflex MALDI–TOF mass spectrometer (Bremen, Germany), operated in positive reflectron and linear mode with a 337 nm of nitrogen laser for desorption/ionization of analytes with an accelerating voltage of 20 kV for accelerating ions into the mass analyzer. The sample "sweet spots" were irradiated with nitrogen laser by observing with camera, which felicitate to obtain good mass spectra with high signal intensities. Each MALDI mass spectrum was generated by an average of 200 laser shots. The mass resolution is defined as $m/\Delta m_{50\%}$, where "m" represents the mass of analytes and Δm is the peak full width at half maximum amplitude of the sodiated ions at m/z 785 and 696 Da are 4675 for PS ($[16:0/18:1\text{-PS}+Na]^+$) and 4478 for PA ($[16:0/18:1\text{-PA}+Na]^+$), respectively. We also calculated the mass resolution of the singly-charged water-insoluble ATPase proteolipid ion at m/z 8282 Da and the result is 2578.

3. Results and discussion

3.1. Characterization of HOA-modified $BaTiO_3$ NPs

Fig. 1a shows a schematic procedures of the HOA molecules modified on the $BaTiO_3$ NPs. Fig. 1b displays the dispersion ability of unmodified $BaTiO_3$ NPs (as received from Sigma-Aldrich) in aqueous phase. To improve the hydrophilic nature of the $BaTiO_3$ NPs, we treated the $BaTiO_3$ NPs surfaces with H_2O_2 for enhancement of hydrophilic nature by forming more hydroxyl groups on the surfaces of $BaTiO_3$ NPs (Fig. 1c). Fig. 1d reveals that the nature and the dispersion ability of $BaTiO_3$ NPs were completely changed from hydrophilic to hydrophobic after the functionalization of the $BaTiO_3$ NPs surfaces with the HOA molecules. Therefore, the HOA-modified $BaTiO_3$ NPs migrated from aqueous phase to organic phase (Fig. 1b–d).

Fig. 2a and b presents the comparison of the FT-IR spectra of H_2O_2-treated and untreated $BaTiO_3$ NPs. It can be noticed that only two absorption bands at 1432 and 592 cm^{-1} were observed in the FT-IR spectrum of $BaTiO_3$ NPs (Fig. 2b). The peak at 1432 cm^{-1} belongs to the stretching vibrations of carbonate ion ($-CO_3^{2-}$), which is originated from barium carbonate in $BaTiO_3$ NPs. The peak at 592 cm^{-1} corresponds to the Ti–O stretching vibration of $BaTiO_3$ NPs [36–38] and a broad (weak) peak at 3345 cm^{-1} represents the stretching of hydroxyl group. Meanwhile, several peaks at 1300–1700 cm^{-1} corresponded to the H–O–H bending vibrations of H_2O_2-treated $BaTiO_3$ NPs (Fig. 2a). These peaks are formed due to the physically adsorbed water onto the surfaces of NPs. Importantly, the intense peak at 3345 cm^{-1} is due to the hydroxyl group stretching of H_2O_2-treated $BaTiO_3$ NPs (Fig. 2a). Among the FT-IR spectra of H_2O_2-untreated and -treated $BaTiO_3$ NPs, the H_2O_2-treated $BaTiO_3$ NPs FT-IR spectrum showed a strong

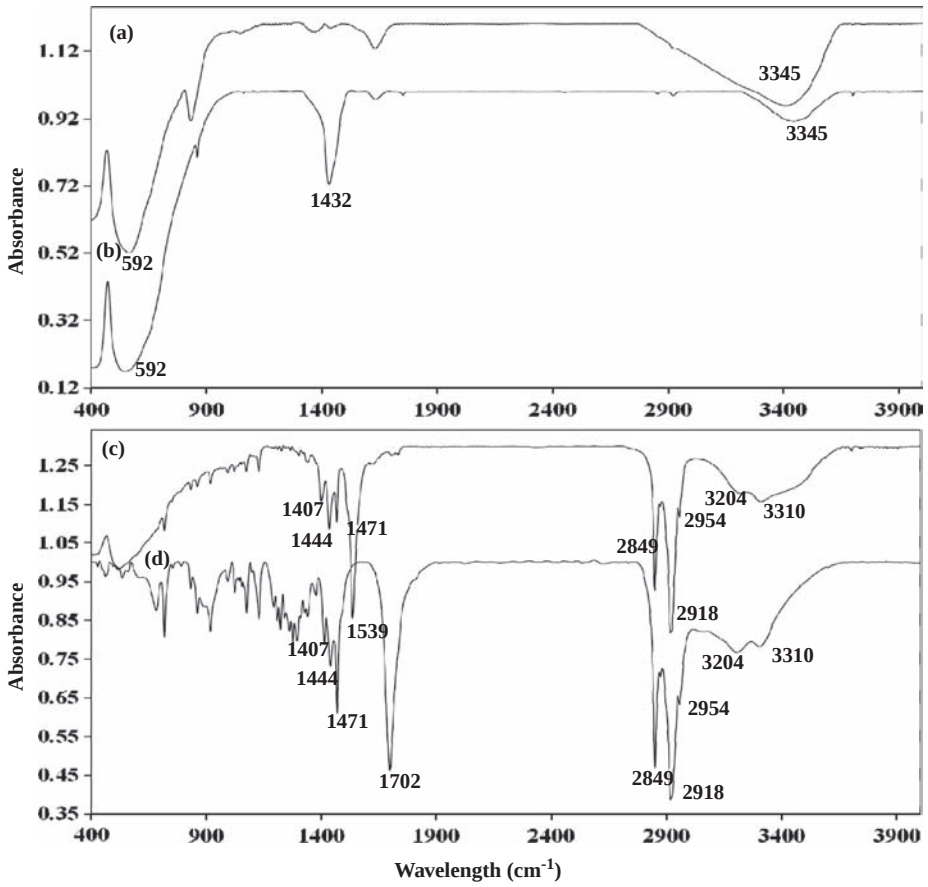

Fig. 2. FT-IR spectra of (a) H_2O_2-treated $BaTiO_3$ NPs, (b) as received $BaTiO_3$ NPs, (c) HOA-modified $BaTiO_3$ NPs and (d) pure HOA.

and broadband peak of –OH stretching peak at 3345 cm^{-1}, which confirms more –OH groups were generated onto the surfaces of $BaTiO_3$ NPs. To demonstrate the surface reactivity of the H_2O_2-treated $BaTiO_3$ NPs, we modified the $BaTiO_3$ NPs surfaces with HOA. Fig. 2d shows the FT-IR spectrum of pure HOA. The peaks at 2849, 2918 and 2954 cm^{-1} correspond to $–CH_2$, $–CH_3$ and C–H groups which are the symmetric, antisymmetric and asymmetric stretching vibrations, respectively. The peak at 1702 cm^{-1} represents the stretching vibrations of carbonyl (C=O) group of carboxylic acid.

Furthermore, stretching vibrations of both –OH groups (alcohol group and carboxylic acid groups) were observed at 3204 and 3310 cm^{-1} (Fig. 2d). While the 3204 cm^{-1} peak was almost disappear after functionalization of $BaTiO_3$ NPs surfaces with HOA (Fig. 2c). These results reveal that the strong interaction between –COOH group of HOA and –OH group of $BaTiO_3$ NPs. Moreover, peaks at 1471, 1444 and 1407 cm^{-1} represent asymmetric $\nu_{as}(COO^-)$ and symmetric $\nu_s(COO^-)$ stretching of carboxylate (Fig. 2c, d). Note that asymmetric and symmetric stretching peaks of carboxylate ions were shifted from 1702 cm^{-1} to 1539 cm^{-1} by the reaction of –COOH group of HOA with –OH group of $BaTiO_3$ NPs (Fig. 1a). Thus, the differences between asymmetric $\nu_{as}(COO^-)$ and symmetric $\nu_s(COO^-)$ stretching peaks were observed at 68 cm^{-1} for HOA-modified $BaTiO_3$ NPs (1539−1471 = 68 cm^{-1}; Fig. 2c) and at 231 cm^{-1} for pure HOA (1702−1471 = 231 cm^{-1}; Fig. 2d) [39,40]. Importantly, a strong intense peak at 1539 cm^{-1} belongs to the vibrations of carboxylates ($–COO^-$), which confirms the bond formation between –COOH group of HOA and –OH group of $BaTiO_3$ NPs (Fig. 2c). Based on these observations, HOA molecules were successfully attached on the surfaces of $BaTiO_3$ NPs through bidentate-type bonding (Fig. 1a). Meanwhile, the peak intensity of –OH group stretching vibrations of HOA-modified $BaTiO_3$ NPs greatly decreased when compared with the peak intensity of H_2O_2-treated $BaTiO_3$ NPs (Fig. 2a and c). These results confirm that the hydroxylation of $BaTiO_3$ NPs plays a key role for the functionalization of $BaTiO_3$ NPs with HOA, which is responsible to change their dispersion ability and nature.

We also studied the morphology and sizes of $BaTiO_3$ NPs and HOA-modified $BaTiO_3$ NPs by SEM and TEM. The SEM images of bare $BaTiO_3$ NPs and HOA-modified $BaTiO_3$ NPs are shown in Fig. 3a, b. It can be observed that the both $BaTiO_3$ NPs have similar morphology. The morphology and sizes of bare $BaTiO_3$ NPs and HOA-modified $BaTiO_3$ NPs were further investigated by TEM (Fig. 3c, d). These results clearly indicate that the bare $BaTiO_3$ NPs and HOA-modified $BaTiO_3$ NPs were well dispersed in solution and the sizes of bare $BaTiO_3$ NPs and HOA-modified $BaTiO_3$ NPs were found to be 30–40 nm. Moreover, the HOA molecules form uniformly layers on the surface of $BaTiO_3$ NPs (Fig. 3d) and they are also well dispersed in toluene (Fig. 1d).

3.2. Dual functions of the HOA-modified $BaTiO_3$ NPs in MALDI–MS

The dual roles of the HOA-modified $BaTiO_3$ NPs to act as the matrix and extracting probes are demonstrated in PLs (PS and PA) analysis by MALDI–MS. The structures of PS and PA are shown in Figs. 4 and 5. PS and PA molecules are containing saturated (C16:0 indicates 16 carbon chains with zero unsaturated bond) and unsaturated alkyl chains (C18:1 signifies an 18 carbon chains with one unsaturated bond) on the monoglyceride phosphate group along with serine group. In this view, the MALDI–MS might be difficult to study the quantitative information of PLs by using solid matrices [41] since the PLs contain a hydrophobic tail and a hydrophilic headgroup, which makes them difficult to dissolve in aqueous solution. To overcome this difficulty, we used HOA-modified $BaTiO_3$ NPs as

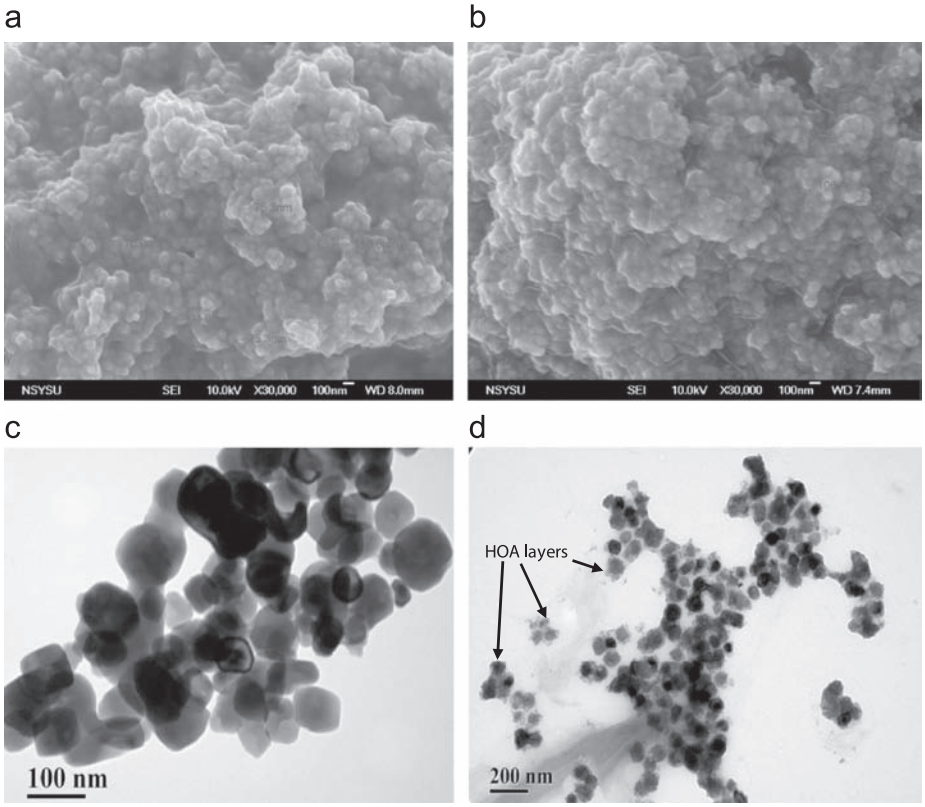

Fig. 3. SEM images of (a) as received $BaTiO_3$ NPs and (b) HOA-modified $BaTiO_3$ NPs, TEM images of (c) as received $BaTiO_3$ NPs and (d) HOA-modified $BaTiO_3$ NPs.

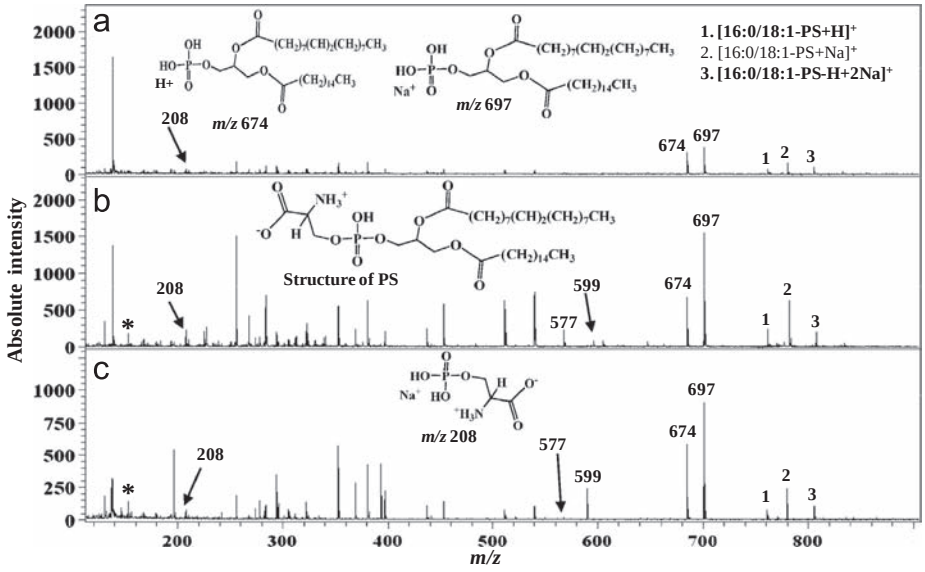

Fig. 4. MALDI mass spectra of PS (2.0 μM) by using (a) HOA-modified $BaTiO_3$ NPs as the liquid matrix, (b) 2,5-DHB as the matrix along with HOA-modified $BaTiO_3$ NPs and (c) 2,5-DHB as the matrix, The mass peaks at *m/z* 764, 785 and 808 are corresponded to $[16:0/18:1\text{-PS+H}]^+$, $[16:0/18:1\text{-PS+Na}]^+$ and $[16:0/18:1\text{-PS+2Na-H}]^+$, respectively.

the bifunctional nanoprobes (as the matrix and as extracting probes) for PLs analysis in MALDI–MS. Fig. 4a shows the MALDI mass spectrum of PS by using HOA-modified $BaTiO_3$ NPs as extracting probes and as the liquid matrix. In this mass spectrum, several ions appeared as protonated $[16:0/18:1\text{-PS+H}]^+$, sodiated $[16:0/18:1\text{-PS+Na}]^+$and disodiated $[16:0/18:1\text{-PS+2Na-H}]^+$ adduct ions at *m/z* 764, 785 and 808, respectively. It is noticed that the significant reduction in PS peaks can be observed in direct MALDI–MS analysis. To improve the signal intensities of PS, we mixed 0.5 M of 2,5-DHB with PS conjugated HOA-modified $BaTiO_3$ NPs (Fig. 4b). This result indicated that the signal intensities of PS were improved by the addition of 2,5-DHB as supporting matrix along with HOA-modified $BaTiO_3$ NPs, which acts as an external proton donor to enhance the signal intensities of analytes. However, matrix cluster ions were observed and showed with asterisks. Fig. 4c indicates the MALDI mass spectrum of PS by using 2,5-DHB as the traditional matrix without HOA-modified $BaTiO_3$ NPs. The peaks that we observed in the mass spectrum belong to PS. All peaks are identical with the mass spectra of PS by using HOA-modified $BaTiO_3$ NPs and 2,5-DHB with HOA-modified $BaTiO_3$ NPs as matrices. This result confirmed that the HOA-modified $BaTiO_3$ NPs-assisted MALDI–MS approach allows to produce dominant analytes peaks with reduced background signals.

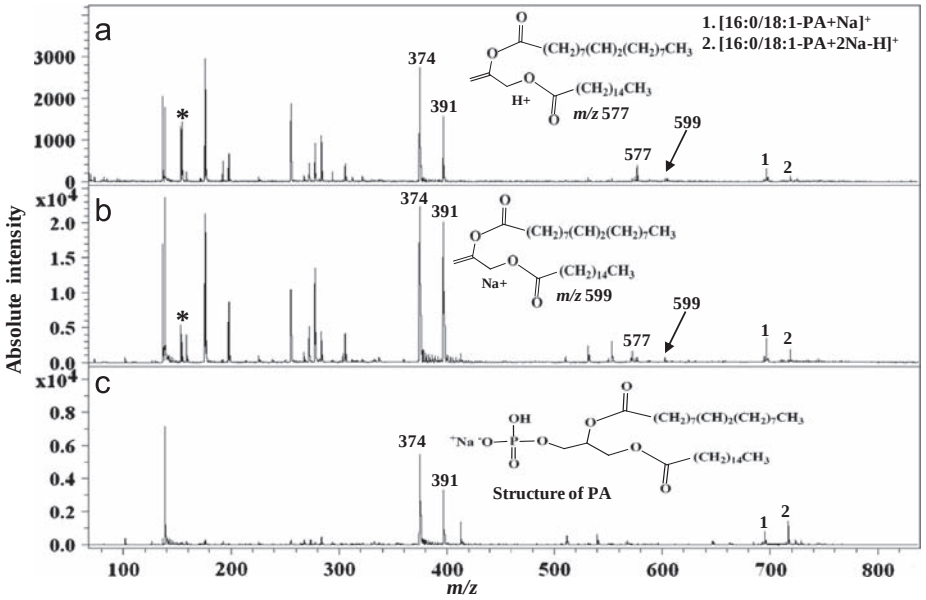

Fig. 5. MALDI mass spectra of PA (2.0 μM) by using (a) 2,5-DHB as the matrix, (b) 2,5-DHB as the matrix along with HOA-modified $BaTiO_3$ NPs and (c) HOA-modified $BaTiO_3$ NPs as the liquid matrix. The mass peaks at *m/z* 696 and 719 are corresponded to $[16:0/18:1\text{-PA+Na}]^+$ and $[16:0/18:1\text{-PA+2Na-H}]^+$, respectively.

As it can be seen in Fig. 4b, c, two mass peaks at *m/z* 696 and 674 were generated with high signal intensities by the loss of headgroup (serine group, 106 Da) from the mass peaks of $[16:0/18:1\text{-PS+H}]^+$ and $[16:0/18:1\text{-PS+Na}]^+$, respectively. Furthermore, it also contains three fragmented mass peaks at *m/z* 599, 577 and 208 which corresponded to adducts ions (protonated and sodiated) of aceylglycerol portions in PS and polar headgroup (serine and phosphate group). The fragmented structures of PS were shown in Fig. 4. Fig. 5a shows the MALDI mass spectrum of PA by using 2,5-DHB as the traditional matrix. In this mass spectrum, sodiated and disodiated ions of PA were observed at *m/z* 696 and 719, which corresponded to $[16:0/18:1\text{-PA+Na}]^+$ and $[16:0/18:1\text{-PA+2Na-H}]^+$, respectively. Apart from these peaks, we also observed the mass peaks at *m/z* 599, 577, 391 and 374 which are due to the loss of serine and phosphate groups from PA. The same mass peaks were observed when we used 2,5-DHB along with HOA-modified $BaTiO_3$ NPs (Fig. 5b). Fig. 5c displays the mass spectrum of PA by using HOA-modified $BaTiO_3$ NPs as the liquid matrix. In comparison with 2,5-DHB, less fragmented mass peaks and reduced background noise were observed for PLs by using HOA-modified $BaTiO_3$ NPs. These results revealed that HOA-modified $BaTiO_3$ NPs acted as extracting probes and as liquid matrix for the analysis of PLs by MALDI–MS.

3.3. Analytical data

We also studied the quantification of PS and PA by using 2,5-DHB, 2,5-DHB along with HOA-modified $BaTiO_3$ NPs and HOA-modified $BaTiO_3$ NPs as the matrices and the obtained analytical data are shown in Table 1. The calibration curves demonstrate good linearity within the range of 1.0–5.0 μM and 1.0–10.0 μM for PS and PA by using the above matrices (Fig. S1). The number of experimental points taken for regression curve was $n=5$ (1.0–5.0 μM) for PS and $n=10$ (1.0–10.0 μM) for PA, respectively. To fit calibration curve accurately, we constructed calibration graph by taking 10 points ranging from 1.0 μM to 10.0 μM for PA. The correlation coefficients (R^2) were found to be 0.9967, 0.9912 and 0.9980 for PS and 0.9987, 0.9905 and 0.9976 for PA, respectively. The recoveries of these analytes (PS and PA) are in the range of 96.6%–99.4% with the relative standard deviation (RSD; $n=5$) values $<6.7\%$. To minimize the analytical errors, we calculated the detection limit by measuring S/N at three times from the mean of the blank concentration and the standard deviation of the blank ($n=5$). The limits of detections (LODs) were found to be 0.20–0.35 μM and 0.25–0.40 μM for PS and PA, respectively. Fig. S2 represents the MALDI mass spectrum of PA (5.0 μM) by using HOA-modified $BaTiO_3$ NPs as the liquid matrix. These results demonstrated that the HOA-modified $BaTiO_3$ NPs could be successfully used as the matrix and as affinity probes for the analysis of PLs in MALDI–MS. Since the HOA molecules modified on the surface of $BaTiO_3$ NPs can reduce the polarity and increase the hydrophobic nature due to the long alkyl chains of HOA (Fig. 1a). Therefore, the hydrophobic interactions are involved between the HOA-modified $BaTiO_3$ NPs and the alkyl chains of PLs, which facilitate to absorb or trap PLs from sample solution. Meanwhile, we also assessed that the higher hydrophobicity of HOA-modified $BaTiO_3$ NPs tends to increase the target species concentration onto the surfaces of $BaTiO_3$ NPs through hydrophobic interactions, which enhances the ionization of the analyte ions in the mass spectra [42]. The hydrophobicity and dispersion ability of $BaTiO_3$ NPs allow to penetrate the molecules on $BaTiO_3$ NPs surfaces, and therefore, the efficiency of laser energy transferred from NPs to analytes is enhanced. The HOA-modified $BaTiO_3$ NPs-assisted MALDI–MS is a promising tool for the analysis of PLs in biological samples. Table 2 illustrates the comparison of the present method with the

Table 1
Analytical data for the analysis of PLs using HOA-modified $BaTiO_3$ NPs-assisted MALDI–MS.

Analytical data	Analytes					
	PS $[16:0/18:1\text{-PS+Na}]^+$			PA $[16:0/18:1\text{-PA+Na}]^+$		
	2,5-DHB	HOA–$BaTiO_3$ NPs	2,5-DHB+ HOA–$BaTiO_3$ NPs	2,5-DHB	HOA–$BaTiO_3$ NPs	2,5-DHB +HOA–$BaTiO_3$ NPs
Linear range (μM)	1.0–5.0	1.0–5.0	1.0–5.0	1.0–10.0	1.0–10.0	1.0–10.0
Regression (R^2)	0.9967	0.9912	0.9980	0.9987	0.9905	0.9976
LOD (μM)	0.35	0.35	0.20	0.40	0.40	0.25

Table 2
Comparison of HOA-modified $BaTiO_3$ NPs-based MALDI–MS for the detection of PLs with MALDI–MS and IMS methods in literature.

Name of the matrix	Name of PLs	Detection limit	Type of MS	Reference
4-Nitroaniline/butyric acid	PC, PG, PA, PS and DMPC	–	MALDI–MS	[16]
BA-CHCA and MI-CHCA	PC, PA, PE, PS and PG	~100 ng/μL and ~100 μg/μL	MALDI–MS	[18]
2,5-DHB, SA, CHCA and esculetin	PC, PE, PS, PG and PA	0.5 pM	MALDI–MS	[19]
CHCA-butylamine and 2,5-DHB-butylamine	PE, PS and PC	500–40 fM	MALDI–IMS	[21]
2,5-DHB	PC	–	MALDI–IMS	[22]
2,5-DHB and CHCA along with piperidine	PI and PC	–	MALDI–IMS	[23]
DAPI, DHAP and 2,5-DHB	PMPC, DPPC, PAPC, PC, PDoPC, PE, PG, PI, PLPG, PMPC, POPC, POPG, PPG, and PS	–	ESI–, MALDI–MS, MALDI–IMS	[24]
2,5-DHB	PC, PE, PI, PA, PG and PS	–	MALDI–IMS	[25]
HOA–$BaTiO_3$ NPs along with 2,5-DHB	PS and PA	0.20–0.40 μM	MALDI–MS	Present work

PC—phosphatidylcholine; PG—phosphatidylglycerol; PA—phosphatidic acid; DMPC—dimyristoyl phosphatidylcholine; PE—phophatidylethanolamine; PI—phosphotidylinositol; PM-PC—palmitoyl-myristoyl-PC; DPPC—dipalmitoyl-PC; PAPC—palmitoyl-arachidonoyl-PC; PDoPC—palmitoyl-docosahexaenoyl-PC; PLPG—palmitoyl-linoleoyl-PG; POPC—palmitoyl-oleoyl-PC; POPG—palmitoyl-oleoyl-PG; PPG—polypropylene glycol.

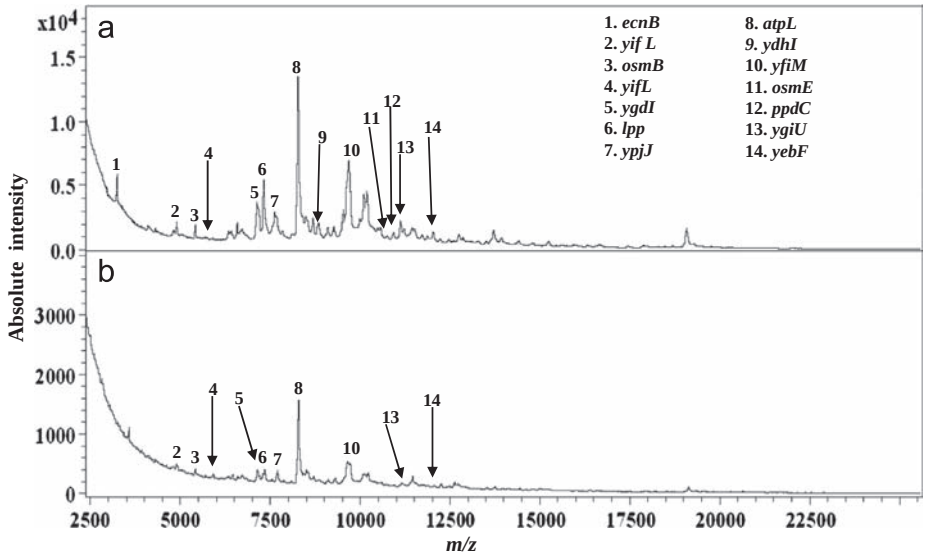

Fig. 6. MALDI mass spectra of identified hydrophobic proteins in *E. coli* by using (a) HOA-modified $BaTiO_3$ NPs-assisted LLME along with SA (0.5 M) as the matrix and (b) SA (0.5 M) as the matrix without HOA-modified $BaTiO_3$ NPs. The details of identified hydrophobic proteins of *E. coli* were depicted in Table 2.

reported ESI–, MALDI–MS and MALDI–IMS methods for the analysis of PLs in literature.

3.4. HOA-modified $BaTiO_3$ NPs-assisted LLME of hydrophobic proteins in E. coli

To investigate the potential applications of HOA-modified $BaTiO_3$ NPs, we applied these NPs as extracting and preconcentrating probes for LLME of hydrophobic proteins in *E. coli* prior to their identification by MALDI–MS. After culturing *E. coli*, the plate count method was used for the enumeration of total bacteria in the culture. The bacterial count in each sample vial was 1.5×10^8 cfu/mL. The sample vials were ultrasonicated to break the bacteria cells and to release more proteins into the sample solutions, which can enhance the bacteria proteins signals in MALDI–MS. Fig. 6a shows the MALDI mass spectrum of identified hydrophobic proteins in *E. coli* by using HOA-modified $BaTiO_3$ NPs-assisted LLME coupled with MALDI–MS. It was noticed that 14 hydrophobic proteins were successfully extracted and preconcentrated by using HOA-modified $BaTiO_3$ NPs as hydrophobic affinity probes. Importantly, the signal intensities of hydrophobic proteins (at *m/z* 5090, 5368, 7009, 7173, 7861 and 8405) were greatly enhanced (2–13 times) by using HOA-modified $BaTiO_3$ NPs as extracting and preconcentrating probes. The generated mass peaks at *m/z* 3418, 7185, 10,855, 5878, and 7020 Da corresponded to the membrane proteins *ecnB* (P56549), *lpp* (P69776), and *osmE* (P23933) and to hypothetical membrane proteins *yifL* (P39166) and *ygdI* (P65292), respectively.

Furthermore, acetyl–acyl carrier protein (*ydhI*; acetyl-ACP, P0A6A8; acetylation of the phosphopantetheine sulfur) was also detected at *m/z* 8888 [43]. Evidently, it can be noticed that five lipoproteins (*ecnB, lpp, osmE, yifL, ygdI*) and water-insoluble ATPase proteolipid (at *m/z* 8282; *atpL*, P68699) were effectively extracted, preconcentrated and then identified by using HOA-modified $BaTiO_3$ NPs-LLME coupled with MALDI–MS. At the same time, we also studied the direct MALDI mass spectrum of *E. coli* (1.5×10^8 cfu/mL) by using SA (0.5 M) as the matrix (Fig. 6b). Unfortunately, only one peak (at *m/z* 8405) is generated with good signal intensity, remaining peaks (2, 3, 4, 5, 6, 7, 13 and 14) are not well resolved and some of the peaks (1, 9, 11 and 12) are not generated by using SA as the matrix. Based on the above results, we confirmed that HOA-modified $BaTiO_3$ NPs have showed high affinity towards hydrophobic proteins of *E. coli*. The identified hydrophobic proteins and their *m/z* values are depicted in Table 3.

Table 3
Identified hydrophobic proteins in *E. coli* by HOA-modified $BaTiO_3$ NPs-assisted LLME coupled with MALDI–MS.

Peak no.	Protein name	Observed *m/z*	Theoritical *m/z*	Access. no.[a]
1	*ecnB*	3418	3409	P56549
2	*yifL*	5090	5099	P39166
3	*osmB*	5360	5368	P0ADA7
4	*yifL*	5878	5887	P39166
5	*ygdI*	7020	7009	Q46924
6	*lpp*	7185	7173	P69776
7	*ypjJ*	7850	7861	P58033
8	*atpL*	8285	8284	P68699
9	*ydhI*	8888	8890	P64471
10	*yfiM*	9925	9931	P46126
11	*osmE*	10,855	10,849	P23933
12	*ppdC*	10,950	10,959	P08372[b]
13	*ygiU*	11,240	11,232	Q46865
14	*yebF*	12,157	12,163	P33219

[a] Hydrophobic proteins are identified as per the literature [43].
[b] Mature protein, but w/o predicted methylation.

It is obvious that HOA molecules on the surfaces of $BaTiO_3$ NPs have played a fundamental key role for the efficient LLME of hydrophobic proteins in *E. coli.* Since, $BaTiO_3$ NPs have attained hydrophobic nature by the functionalization of $BaTiO_3$ NPs surfaces with HOA (17-alkyl chains), which facilitates to enhance the analytes extraction and preconcentration through hydrophobic interactions. The use of HOA in MALDI–MS highly improves its performance by acting as affinity probes and possibly as a "buffer" in laser energy transfer to enhance the desorption/ionization of hydrophobic proteins. These results confirmed that HOA-modified $BaTiO_3$ NPs has great potentiality to use them as hydrophobic affinity probes for LLME of hydrophobic proteins from the biological samples. Based on the above results, HOA-modified $BaTiO_3$ NPs efficiently acted as extracting and concentrating probes for the analysis of hydrophobic proteins in *E. coli* by MALDI–MS.

4. Conclusions

For the first time, we have described the dual roles of HOA-modified $BaTiO_3$ NPs as the matrix and as extracting probes for the analysis of PLs in MALDI–MS. HOA-modified $BaTiO_3$ NPs were used as hydrophobic affinity probes for LLME of hydrophobic proteins from *E. coli* prior to MALDI–MS analysis. This method provides good linearity for the efficient analysis of PLs (PS and PA). Meanwhile, the use of HOA-modified $BaTiO_3$ NPs as the liquid matrix has a paramount impact on the quality of achievable MALDI mass spectra of PLs. The signal intensities of hydrophobic proteins were greatly increased by using HOA-modified $BaTiO_3$ NPs as extracting probes. We believe that this new class of HOA-modified $BaTiO_3$ NPs can potentially be applied as extracting probes and as the matrix for the analysis of PLs and hydrophobic proteins in the biological samples prior to their identification by MALDI–MS.

Acknowledgment

This work was funded by the National Science Council (NSC) of Taiwan. Dr. Suresh Kumar Kailasa thanks NSC for fellowship and the S.V. National Institute of Technology, Surat, India for permission of leave to carry out this work at Department of Chemistry, National Sun Yat-Sen University. Dr. Judy Gopal and Dr. Nazim Hasan (Department of Chemistry, National Sun Yat-Sen University) are acknowledged for assistance in preparing the bacteria samples.

Appendix A. Supporting information

Supplementary information associated with this article can be found in the online version at http://dx.doi.org/10.1016/j.talanta.2013.05.032.

References

[1] J.A. Glomset, J. Lipid Res. 9 (1968) 155–167.
[2] S. Acton, A. Rigotti, K.T. Landschulz, S. Xu, H.H. Hobbs, M. Krieger, Science 271 (1996) 518–520.
[3] T.R. Pettitt, A. Martin, T. Horton, C. Liossis, J.M. Lord, M.J. Wakelam, J. Biol. Chem. 272 (1997) 17354–17359.
[4] M.N. Hodgkin, T.R. Pettitt, A. Martin, M.J. Wakelam, Biochem. Soc. Trans. 24 (1996) 991–994.
[5] V.P. Skipski, R.F. Peterson, M. Barclay, Biochem. J. 90 (1964) 374–378.
[6] R. Szucs, K. Verleysen, G.S.M.J.E. Duchateau, P. Sandra, B.G.M. Vandeginste, J. Chromatogr. A 738 (1996) 25–29.
[7] K. Verleysen, P. Sandra, J. High Resolut. Chromatogr. 20 (1997) 337–339.
[8] M. Yamashita, J.B. Fenn, J. Phys. Chem. 88 (1984) 4451–4459.
[9] M. Karas, F. Hillenkamp, Anal. Chem. 60 (1988) 2299–3001.
[10] K. Tanaka, H. Waki, Y. Ido, S. Akita, Y. Yoshida, T. Yoshida, Rapid Commun. Mass Spectrom. 2 (1988) 151–153.
[11] S. Sauer, M. Kliem, Nat. Rev. 8 (2010) 74–82.
[12] C.H. Chen, Anal. Chim. Acta 624 (2008) 16–36.
[13] O.L. Jackson Jr., Mass Spectrom. Rev. 20 (2001) 172–194.
[14] L.F. Marvin, M.A. Roberts, L.B. Fay, Clin. Chim. Acta 337 (2003) 11–21.
[15] Y. Kim, S.R. Shanta, L.H. Zhou, K.P. Kim, Exp. Mol. Med. 42 (2010) 1–11.
[16] B.M. Ham, J.T. Jacob, R.B. Cole, Anal. Chem. 77 (2005) 4439–4447.
[17] H. Hidaka, N. Hanyu, M. Sugano, K. Kawasaki, K. Yamauchi, T. Katsuyama, Ann. Clin. Lab. Sci. 37 (2007) 213–221.
[18] Y.L. Li, M.L. Gross, F.F. Hsu, J. Am. Soc. Mass Spectrom. 16 (2005) 679–682.
[19] J.D. Harvey, J. Mass Spectrom. 30 (1995) 1333–1346.
[20] N. Zaima, T. Hayasaka, N.G. Inoue, M. Setou, Int. J. Mol. Sci. 11 (2010) 5040–5055.
[21] K. Shrivas, T. Hayasaka, N.G. Inoue, Y. Sugiura, N. Zaima, M. Setou, Anal. Chem. 82 (2010) 8800–8806.
[22] S.M. Puolitaival, K.E. Burnum, D.S. Cornett, R.M. Caprioli, J. Am. Soc. Mass Spectrom. 19 (2008) 882–886.
[23] S.H. Shanta, L.H. Zhou, Y.S. Park, T.H. Kim, Y. Kim, K.P. Kim, Anal. Chem. 83 (2011) 1252–1259.
[24] K.A. Berry, B. Li, S.D. Reynolds, R.M. Barkley, M.A. Gijon, J. Hankin, P.M. Henson, R.C. Murphy, J. Lipid Res. 52 (2011) 1551–1560.
[25] R.C. Murphy, J.A. Hankin, R.M. Barkley, J. Lipid Res. 50 (2009) S317–S322.
[26] Z. Guo, A.A.A. Ganawi, Q. Liu, L. He, Anal. Bioanal. Chem. 384 (2006) 584–592.
[27] C.K. Chiang, W.T. Chen, H.T. Chang, Chem. Soc. Rev. 40 (2011) 1269–1281.
[28] P.R. Sudhir, K. Shrivas, H.F. Wu, Z.C. Zhou, Rapid Commun. Mass Spectrom. 22 (2008) 3076–3086.
[29] S.K. Kailasa, H.F. Wu, Analyst 137 (2012) 4490–4496.
[30] P.R. Sudhir, H.F. Wu, Z.C. Zhou, Anal. Chem. **77** (2005) 7380–7385.
[31] L. Shastri, S.K. Kailasa, H.F. Wu, Talanta 81 (2010) 1176–1182.
[32] S.K. Kailasa, H.F. Wu, Talanta 83 (2010) 527–534.
[33] G. Ciofani, S. Danti, D. D'Alessandro, S. Moscato, M. Petrini, A. Menciassi, Nanoscale Res. Lett. 5 (2010) 1093–1101.
[34] T.R. Northen, O. Yanes, M.T. Northen, D. Marrinucci, W. Uritboonthai, J. Apon, S. L. Golledge, A. Nordström, G. Siuzdak, Nature 449 (2007) 1033–1036.
[35] J.P. Harley, L.M. Prescott, Laboratory Exercises in Microbiology, 5th ed., McGraw-Hill Science, New York, 1996.
[36] S.J. Chang, W.S. Liao, C.J. Ciou, J.T. Lee, C.C. Li, J. Colloid Interface Sci. 329 (2009) 300–305.
[37] H.A. Al-Abadleh, H.A. Al-Hosney, V.H. Grassian, J. Mol. Catal. A: Chem. 228 (2005) 47–54.
[38] P. Kim, S.C. Jones, P.J. Hotchkiss, J.N. Haddock, B. Kippelen, S.R. Marder, J.W. Perry, Adv. Mater. 19 (2007) 1001–1005.
[39] C.C. Li, M.W. Chang, Mater. Lett. 58 (2004) 3903–3907.
[40] G. Socrates, Infrared Characteristic Group Frequencies—Tables and Charts, Second ed., Wiley, New York, 1994.
[41] M. Mank, B. Stahl, G. Boehm, Anal. Chem. 76 (2004) 2938–2950.
[42] J. Duan, M.J. Linman, Q. Cheng, Anal. Chem. 82 (2010) 5088–5094.
[43] R.R.O. Loo, J.A. Loo, Anal. Chem. 79 (2007) 1115–1125.